TMT tertiary mirror axis calibration with laser tracker*

AN Qi-chang (安其昌)**, **ZHANG Jing-xu** (张景旭), **YANG Fei** (杨飞), **and SUN Jing-wei** (孙敬伟)
Changchun Institute of Optics, Fine Mechanics and Physics, Chinese Academy of Sciences, Changchun 130033, China

(Received 28 January 2015)

To calibrate the tracing performance of the thirty meter telescope (TMT) tertiary mirror, for the special requirement of the TMT, the laser tracker is used to verify the motion. Firstly, the deviation is divided into two parts, namely, the repeatable error and the unrepeatable part. Then, based on the laser tracker, the meartурement and evalutation methods of the rigid body motion for the mirror are established, and the Monte Carol method is used to determine the accuracy of the mothod. Lastly, the mothod is applied to the turn table of a classical telescope and the residual error is about 4 arc second. The work of this paper will guide the next desgin and construction work of the thirty meter telescope tertiary mirror.
Document code: A **Article ID:** 1673-1905(2015)02-0084-4
DOI 10.1007/s11801-015-5019-9

The thirty meter telescope (TMT) is one of the largest telescopes in the world, which is built in Hawaii. As a Ritchey-Chrétien system, the main mirror is composed of 492 hexagonally-shaped hyperboloid segments that remain co-phased. The tertiary mirror is a flat reflecting mirror with 3.594 m by 2.576 m elliptical shaped[1-3].

The tertiary mirror is very challenging because it directs the beam to the instrument on the both sides of the elevator axis during the tracking of the telescope. For the extremely high level of pointing accuracy, the calibration of the beam that comes out from the mirror is very important[4-6].

The tertiary mirror is mounted in a positioner assembly which provides rigid body rotation and tilt. The system is developed by the Changchun Institute of Optics, Fine Mechanics and Physics in Changchun of China.

As the TMT requires, the calibration of the both axes is under the consideration of the whole coordination. It means that the error in every part of the tertiary mirror is accumulated to the tilt and rotation motion of the mirror. The error of the encoder, the noise in the control close loop, the fabrication error of the structure, the gravity sag and the thermal gradient[7-10] are concerned.

The errors can be divided into two kinds: the repeatable error and the unrepeatable error. For the repeatable error, the main source is the gravity sag. In every time of observation, with the gravity vector changing, the structure will deform according to the working conditions. This error can be corrected by the open loop, namely, the look-up table. The unrepeatable one is the major problem in the calibration.

This paper will calibrate the encoder to make sure that the tertiary mirror system will be able to rotate the M3 mirror about tilt/rotation axis to any angle within the ranges from 34° to 50° for tilt and from -180° to 180° for rotation, with a repeatable M3 rotation error (after telescope calibration) of less than 3.5 arc seconds in root mean square (RMS). The calibration will allow component adjustment or replacement if requirements are not met during the motion of each axis at multiple zenith angle orientations. For the challenge of the calibration, we choose the laser tracker as the tool to obtain the rigid motion of the mirror[11,12].

In this paper, the calibration measurement and calculation methods will be discussed. Then the accuracy of the method will be analyzed. And the measurement is applied to a classical telescope turn table, just as the way that it will be applied to the actual tertiary mirror.

The coordinate system in Fig.1 shows the motions in the tertiary mirror system. The calibration focuses on the angular motions in the ECRS-*Z* axis and M3CRS-*X* axis directions, corresponding to the rotation angle θ and tilt angle ϕ.

All the pointing errors are finally evaluated in these directions. As described above, when we calculate the value of the jitter, we should measure the rigid body motion of the mirror itself, and then, project the error on the ECRS-*Z* axis and M3CRS-*X* axis.

For the requirement of the TMT, the rotation/tilt axis of the partially assembled M3PAP will be tested with surrogate weights added to represent missing hardware to measure the motion requirement applied to this axis. The testing will be performed with the rotation axis aligning to the gravity vector and with the rotation axis rotating to one additional angle at least with respect to the gravity vector.

* This work has been supported by the National Natural Science Foundation of China (No.11403022).
** E-mail: anjj@mail.ustc.edu.cn

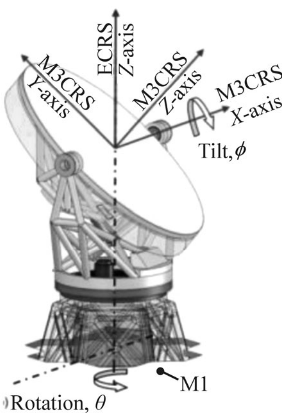

Fig.1 Coordinates of the TMT M3

In order to measure the point error, introduced by gravity sag, thermal expansion, friction ripple, etc., the mirror rigid body location will be tested. The laser tracker is recently involved to measure the large scale distance with high accuracy. The sensor on the mirror is a spheric reflector, which can reflect the laser beam from any direction. It is more convenient to allocate in the different places in the very large system by certain small interface, as shown in Fig.2.

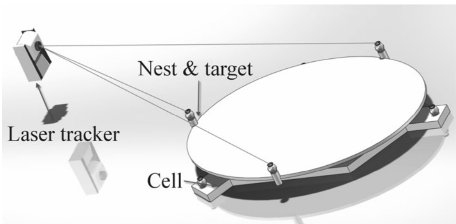

Fig.2 Laser tracker for the TMT M3

As shown in Fig.2, the coordinates of the three targets are achieved by the laser tracker, noted as $[x_1, y_1, z_1]$, $[x_2, y_2, z_2]$, $[x_3, y_3, z_3]$.

The normal vector, M3CRS-*Z* axis is:

$$\boldsymbol{n} = \frac{\boldsymbol{a} \times \boldsymbol{b}}{|\boldsymbol{a}||\boldsymbol{b}|} . \tag{1}$$

This vector can present the point direction of the mirror, where

$$\boldsymbol{a} = [x_1, y_1, z_1] - [x_3, y_3, z_3] ,$$

$$\boldsymbol{b} = [x_2, y_2, z_2] - [x_3, y_3, z_3] . \tag{2}$$

The position of the mirror can be expressed by

$$[c_x, c_y, c_z] = \frac{[x_1, y_1, z_1] + [x_2, y_2, z_2] + [x_3, y_3, z_3]}{3} . \tag{3}$$

The rotation vector about the ECRS-*Z* axis is

$$\boldsymbol{r}_{\text{ECRS}-Z} = \boldsymbol{n} - \boldsymbol{V}_{\text{ECRS}-Z} \cdot \boldsymbol{n} . \tag{4}$$

The rotation vector about the M3CRS-*X* axis is

$$\boldsymbol{r}_{\text{M3CRS}-X} = \boldsymbol{V}_{\text{M3CRS}-X} \times \boldsymbol{n} , \tag{5}$$

where $\boldsymbol{V}_{\text{ECRS}-Z}$ and $\boldsymbol{V}_{\text{M3CRS}-X}$ are the unit direction vectors of the axis. By the vectors, the rotation angle θ and tilt angle ϕ can be calculated.

The Fourier series has already been widely used in the analysis of the shaft, so we employ the technique to analyze the data.

The Fourier series of $w(t)$ is:

$$w(t) = \sum_{n=-\infty}^{\infty} c_n \mathrm{e}^{\mathrm{j}\omega_0 t} =$$

$$\sum_{n=0}^{\infty} a_n \cos n\omega_0 t + \sum_{n=0}^{\infty} b_n \sin n\omega_0 t , \tag{6}$$

where

$$c_n = \frac{1}{T} \int_a^{a+T} w(t) \mathrm{e}^{-\mathrm{j}n\omega_0 t} \,\mathrm{d}t . \tag{7}$$

When $\Delta t = T / N$, we get

$$c_n \approx \frac{1}{T} \int_a^{a+T} w(k\Delta t) \mathrm{e}^{-\mathrm{j}n\omega_0 k\Delta t} \,\mathrm{d}t =$$

$$\frac{1}{T} \sum_{n=0}^{N-1} w(k\Delta t) \mathrm{e}^{-\mathrm{j}nk(2\pi/N)} \Delta t . \tag{8}$$

Note that the fast Fourier translation (FFT) of $w(t)$ is $x(n)$, so $c_n = \frac{1}{N} X(n)$. Then

$$a_n = 2\,\mathrm{Re}(c_n);$$

$$b_n = -2\,\mathrm{Im}(c_n) . \tag{9}$$

For the laser tracker, we can use the points to construct vectors, and then calculate the rotation/tilt angle. Thus, the low order series will be removed, and then the residual rotation/tilt error can be achieved.

In the laser tracker case, the rotation/tilt angles have no equal interval. This will make the fast Fourier transform impossible.

For most cases, the first order interpolation will be adequate for the fitting. The interpolation with too high order polynomials will introduce huge error at the boundary of the testing range.

In the common case, the low order component is always repeatable error. For example, the gravity sag always appears as the sine function. So we should confirm the lower order part to set up the look-up table and then calculate the residual part to make sure that it will meet the requirement.

In most cases, the Gauss-Markov model is used to specify the mathematical relationship between the data and the parameter we want:

$$\begin{cases} \boldsymbol{L} = \boldsymbol{A}\boldsymbol{X} + \boldsymbol{\varDelta} \\ E(\boldsymbol{\varDelta}) = 0; \mathrm{cov}(\boldsymbol{\varDelta}) = \sigma_0^2 \boldsymbol{P}^{-1} \end{cases} , \tag{10}$$

where $\boldsymbol{L}$ is the data matrix, $\boldsymbol{A}$ is the coefficient matrix, X is the parameter to be identified, $\boldsymbol{\Delta}$ is the measurement error, σ_0^2 is the variance, and $\boldsymbol{P}$ is the weight matrix.

The error of identification always comes from two parts: one is the system error due to how the data is collected, and the other is the bias of the estimation method:

$$E\left(\boldsymbol{e}^{\mathrm{T}}\boldsymbol{e}\right)=$$
$$\operatorname{trace}\left[\operatorname{var}\left(\hat{\boldsymbol{x}}\right)\right]+\operatorname{trace}\left\{\left[\operatorname{bias}\left(\hat{\boldsymbol{x}}\right)\right]^{\mathrm{T}}\left[\operatorname{bias}\left(\hat{\boldsymbol{x}}\right)\right]\right\}. \quad (11)$$

We note that $\lambda_1,\lambda_2,\ldots,\lambda_t$ are the singular values of $\boldsymbol{A}^{\mathrm{T}}\boldsymbol{PA}$, then the singular decomposition of $\boldsymbol{A}^{\mathrm{T}}\boldsymbol{PA}$ is:

$$\boldsymbol{Q}^{\mathrm{T}}\boldsymbol{A}^{\mathrm{T}}\boldsymbol{PAQ}=\operatorname{diag}(\lambda_1,\lambda_2,\ldots,\lambda_t), \quad (12)$$

for:

$$\hat{\boldsymbol{x}}_{\mathrm{LS}}=\left(\boldsymbol{A}^{\mathrm{T}}\boldsymbol{PA}\right)^{-1}\boldsymbol{A}^{\mathrm{T}}\boldsymbol{PL}. \quad (13)$$

The error of the estimation is:

$$\operatorname{MSE}\left(\hat{\boldsymbol{X}}_{\mathrm{LS}}\right)=\sigma_0^2\operatorname{trace}\left[\left(\boldsymbol{A}^{\mathrm{T}}\boldsymbol{PA}\right)^{-1}\right]=\sigma_0^2\sum_{i=0}^{t}\lambda_i^{-1}. \quad (14)$$

The residual error always follows the normal distribution, as shown in Fig.3, which is the residual pointing error of a classical telescope. The distribution is very close to the normal one.

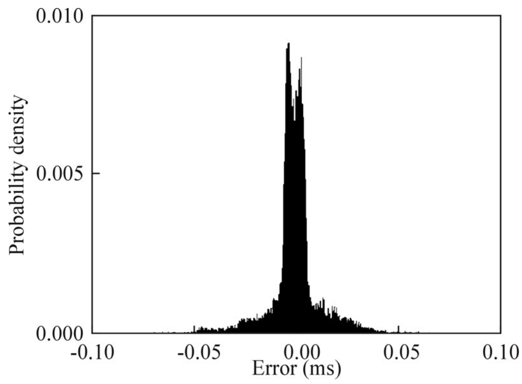

Fig.3 Residual pointing error of a classical telescope

In the sphere coordinates, the three dimensional coordinates of one point can be expressed as follows:

$$\begin{bmatrix} x \\ y \\ z \end{bmatrix}=\begin{bmatrix} l\cos\alpha\sin\beta \\ l\sin\alpha\cos\beta \\ l\cos\beta \end{bmatrix}. \quad (15)$$

We note that the three parameters with error can be expressed as follows:

$$l'=l+\varepsilon_l,$$
$$\alpha'=\alpha+\varepsilon_\alpha,$$
$$\beta'=\beta+\varepsilon_\beta. \quad (16)$$

The length item error is about 0.1 μm, and the encoder is sensitive to the angular motion more than 1″. As is shown before, we suppose that: $\varepsilon_l \sim N(0,0.1)$, $\varepsilon_\alpha \sim N(0,1)$, $\varepsilon_\beta \sim N(0,1)$.

So in this case, considering Eq.(14), we get

$$\operatorname{MSE}\left(\hat{\boldsymbol{X}}_{\mathrm{LS}}\right)=\frac{\sigma_0^2}{r}=\frac{\left(\sigma_x^2,\sigma_y^2,\sigma_z^2\right)\cdot\left(i,j,k\right)}{r}, \quad (17)$$

where $\sigma_x^2,\sigma_y^2,\sigma_z^2$ are the variances in three directions, $\left(i,j,k\right)$ is the direction vector that will be evaluated, and r is the amplification of the rotation vector.

The angular accuracy is related with the displacement measurement accuracy and the rotation radius. We consider the accuracy versus the distance that the tracker target is away from the mirror center, as shown in Figs.4-6.

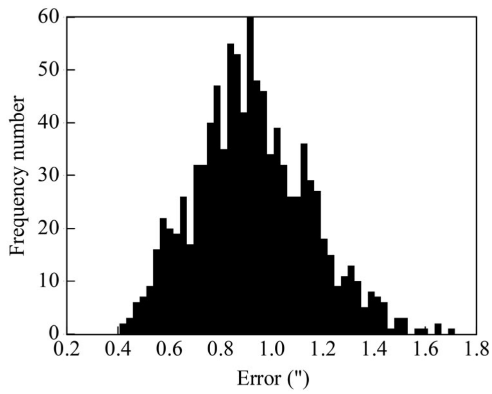

Fig.4 Distribution of the laser tracker testing (*r*=1.9 m)

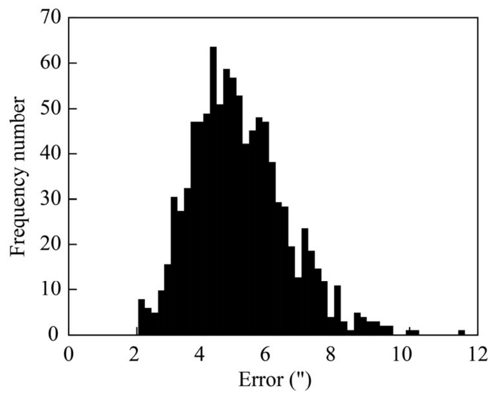

Fig.5 Distribution of the laser tracker testing (*r*=0.5 m)

As shown in the figures, when the mirror is larger than 4 m, the accuracy is less than 1 arc second. If the mirror is smaller, some other fixtures can be used to enlarge the rotation radius.

For the classical telescope, the turn table is a main source of errors in pointing. It is shown in Fig.7 that the turn table is about 1.2 m in diameter, almost 3 m away from the laser tracker. The accuracy is about 1arc second.

Using the method mentioned above, we can obtain the deviation in the normal direction of the axis:

$$\delta\theta_{\mathrm{ECRS-Z}} = \arccos\frac{\boldsymbol{V}_{\mathrm{ECRS-Z}}\cdot\boldsymbol{n}}{|\boldsymbol{n}||\boldsymbol{V}_{\mathrm{ECRS-Z}}|}. \quad (18)$$

We can see from Fig.8 that the first order of sine function is contained in the curve, so it is the repeatable part of the deviation. After it is removed, the residual error is about 4 arc seconds and that should be considered about by the encoder vender or the system controllers.

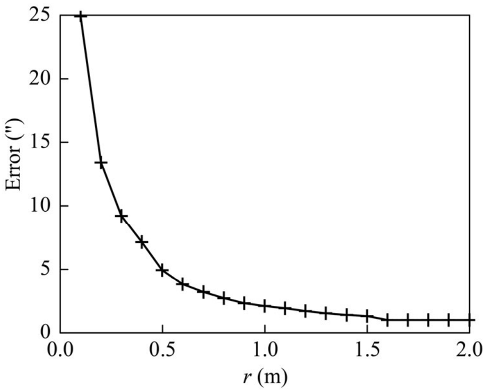

Fig.6 The deviation of the test of laser tracker

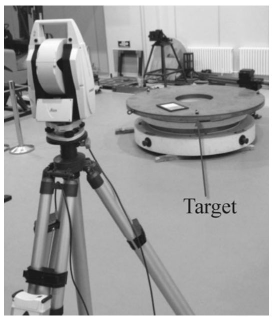

Fig.7 The free response of the mirror system

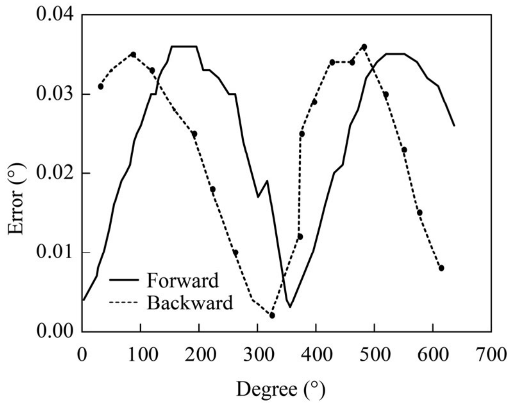

Fig.8 Real part of the transfer function of the mirror system

The calibration test will help to select the components to meet the motion requirements. The system is analyzed to predict the motion, and then the analysis is verified through testing. An understanding of the TMT definition of telescope calibration is achieved.

The tertiary mirror is supplied by the Changchun Institute of Optics, Fine Mechanics and Physics in Changchun of China. There is a 1/4 scale prototype under construction. Some tests are performed to understand the calibration procedure. Furthermore, for the scale theory, the final residual error metric may be better than 3.5 arc seconds in RMS.

Acknowledgements

The author thanks to Dr. Zhao Hong-chao for providing his valuable suggestion.

References

[1] Wang Fu-guo, Yang Fei and Zhao Hong-chao, Chinese Optics **6**, 643 (2013). (in Chinese)

[2] V. Ford, C. Carter and C. Delrez, Jitter Studies for the Secondary and Tertiary Mirror Systems on the Thirty Meter Telescope, SPIE Advances in Optical and Mechanical Technologies for Telescopes and Instrumentation **9151**, 1 (2014).

[3] CAO Xiao-tao, SUN Tian-yu and ZHAO Yun-long, Chinese Optics **7**, 739 (2014). (in Chinese)

[4] LU Rong-sheng, LI Wan-hong and LAO Da-bao, Optics and Precision Engineering **22**, 2299 (2014). (in Chinese)

[5] D. MacMynowski, C. Blaurock and G. Angeli, Dynamic Analysis of TMT, SPIE Modeling System Engineering and Project Management for Astronomy **7017**, 1 (2008).

[6] SHEN Lin-yong, HUANG Chen-chen and QIAN Jin-wu, Optics and Precision Engineering **22**, 3310 (2014). (in Chinese)

[7] W. Skidmore, T. Travouillon and R. Riddle, Experiments at the W. M. Keck Observatory to Support the Thirty Meter Telescope Design Work, SPIE Ground based and Airborne Telescopes III **7733**, 1 (2010).

[8] YANG Hui-sheng, LI Zhi-lai and XU Hong, Optics and Precision Engineering **22**, 3342 (2014). (in Chinese)

[9] Liu Shu-tian, Hu Rui and Zhou Ping, Optics and Precision Engineering **21**, 1803 (2013). (in Chinese)

[10] D. G. MacMynowski, P. M. Thompson and M. J. Sirota, Analysis of TMT Primary Mirror Control-Structure Interaction, SPIE Modeling System Engineering and Project Management for Astronomy **7017**, 1 (2008).

[11] ZHOU Sen, GUO Yong-cai and GAO Chao, Optics and Precision Engineering **22**, 1524 (2014). (in Chinese)

[12] J. Mayo, Mechanical Jitter Measurement Results for Large Ground-Based Telescopes, SPIE Astronomical Structures and Mechanisms Technology **5495**, 98 (2004).